Experimental Determination of the Volume Change of Pure Salts and Salt Mixtures at their Melting Point

J. P. Petitet,[1] M. Fraiha,[1] R. Tufeu,[1] and B. Le Neindre[1]

Measurements of the melting temperature as a function of pressure for some pure salts ($NaNO_3$, $LiOH$) and salt mixtures (Na_2SO_4–$NaCl$, $NaNO_2$–$NaNO_3$–KNO_3, Li_2SO_4–$NaCl$, $NaCl$–$MgCl_2$) are reported. The experiments were performed up to 250 MPa. From the melting curves, the slopes $(dP/dT)_m^0$ at atmospheric pressure were determined. Finally, using the Clapeyron equation, with the enthalpy of melting taken from the literature, the volume change on melting at atmospheric pressure was determined for each compound.

1. INTRODUCTION

Because of their favorable properties, molten salts should play, in the future, a major role as industrial fluids in the temperature range from 50 to 2000°C. Their thermodynamic properties, for instance, make them suitable for energy storage by sensible or latent heat. Among the required qualities for an energy storage material, large heat of melting and specific heat are evident criteria. Moreover, suitable materials must have a small volume change on melting, or at least, this volume change must be known with a reasonable accuracy.

Data on volume change are necessary in thermal and mechanical engineering. On one hand, large volume changes on melting create cracks and gas pockets during cycles of charge and discharge which affect the thermal efficiency. On the other hand, storage units must be dimensioned accounting for mechanical stretchings due to the freezing of the salt during

---

[1] LIMHP-CNRS, Université Paris-Nord, 93430 Villetaneuse, France.

the time of discharge in the case of storage by latent heat or in the case of accidental freezing. Also, it should be noted that a bad contact of the salt with the metallic walls creates favorable sites for corrosion.

The objective of this study is of an applied nature and consists of developing an indirect measurement method based on the Clapeyron equation, which is particularly suited for the determination of small volume changes on melting. Thus we report measurements of the volume change on melting at atmospheric pressure, of salts and salt mixtures. We selected them in order to have a characteristic group of possible situations of heat storage. $NaNO_3$ melts at low temperature, and most of its thermodynamic properties are well known, which allows the testing of our measurement method. LiOH is well known for its small volume change on melting and is often associated as a storage material with other salts like LiCl or LiF [1, 2]. The eutectic Na_2SO_4–NaCl is an ideal mixture for which the method based on the Clapeyron equation, assuming the additivity of melting enthalpies and molar volume of both components, was tested. The mixture $NaNO_2$–$NaNO_3$–KNO_3 is a typical industrial product commercialized a long time ago. The Li_2SO_4–NaCl mixture behaves as an eutectic; its heat of melting is large and it can be a good storage material. The mixture NaCl–$MgCl_2$ was the object of several thermodynamic studies for the purpose of mass storage and is interesting because of its low cost [3].

2. EXPERIMENTAL METHOD

Among the various methods of measurement of the volume change on melting, the direct method of measuring displacement of the liquid is not adequate for the studies of molten salts for technical reasons (such as high temperature, corrosion). The semidirect method of measurement by the junction of liquid and solid dilatometric curves was extensively used for molten salts [4] but requires a carefully fabricated apparatus. In addition, this method has the disadvantage of adding absolute errors on volumes of the liquid and the solid, which may yield wrong results in the case of small volume changes.

Our method of measurement is based on the Clapeyron equation, which relates the volume change on melting ΔV_m^0 to the entropy of melting ΔS_m^0 as follows:

$$\Delta V_m^0 = \Delta S_m^0 (dT/dP)_m^0 \tag{1}$$

where $(\Delta T/\Delta P)_m$ is the temperature variation as a function of pressure along the melting curve. It is this last quantity that we intended to measure.

The entropy of melting was generally selected from the literature data. It is clear, from the energy storage point of view, that ΔS_m^0 must be large to yield a large enthalpy of melting. It follows that a small volume change on melting can exist only if $(dT/dP)_m^0$ is small. The advantage of this method is that it gives directly the relative error in ΔV, which is a desirable condition for the determination of small volume changes on melting.

The experiment consists of the observation of the melting point of the material under pressure by simultaneously recording the melting plateau and the radial temperature difference between the inside and the outside of the cell. The melting plateau constitutes the measurement by itself and is reproducible within ± 0.4 K at a given pressure. The DTA peaks allow control of the melting phenomena. From the melting curve, $T = f(P)$, the slope at the origin is deduced. For the determination of the slope, we found it appropriate to fit all the melting curves by a spline function. The Clapeyron equation is valid for pure substances and can be generalized for all mixtures that are defined compounds or eutectics [5]. In such a method, difficulties arise because of the need of precise knowledge of the melting entropy at atmospheric pressure. Moreover, these experiments require heavy equipment.

3. EXPERIMENTAL SETUP FOR THE DETERMINATION OF THE MELTING CURVE

We developed an original method of measurement with an internal heating which permits experimentation in the temperature range from 25 to 1000°C.

3.1. Electric Furnace.

The electric furnace, built to work up to 1000°C with an input power of 2.5 kW, is set up inside the high pressure vessel, composed of a stainless steel tube (i.d. 26.5 mm, o.d. 33.3, mm, length 446 mm). Since we used an open cell, a vertical geometry was adopted. Two thermocoax wires of 1 and 3Ω were wound on the stainless steel tube. The power delivered by each resistance could be modified to control longitudinal gradients in the cell. During an experiment, the temperature difference between the top and the bottom of the cell did not exceed 4 K. For the insulation of the furnace, the earlier work of Malbrunot et al. [6] for a similar geometry proved to be very useful. Thus the insulation of the furnace was ensured by an ensemble of nickel foils of 0.05 mm thick, separated by a distance of 0.05 mm. The gas layers enclosed between these foils constituted a good thermal insulation

and permitted a furnace of reasonable size to be set inside the high pressure vessel.

3.2. High Pressure Equipment

The high pressure vessel is of classical design. It is a cylinder made of 819B steel (i.d. 65 mm, o.d. 195 mm, useful length 630 mm). It is externally cooled by a water jacket. Experiments were performed from 0.1 to 250 MPa. Argon was chosen as the compressing fluid. A membrane compressor (Corblin) was used up to 100 MPa, and a piston intensifier generated the higher pressures. The pressure is measured by two Heise gauges (0–150 and 0–500 MPa) used in their respective ranges below and above 150 MPa, with an accuracy of 2×10^{-3} of full scale.

3.3. The Experimental Cell

The experimental cell is a cylindrical capsule made of platinum-10% rhodium, with an opening at the top (2 mm diam hole). This hole is used for filling the cell with the salt and for transmitting the pressure by the compressed gas. Evidently, it would have been preferable to use a tight cell to avoid a direct contact between the compressed gas and the salt.

Some preliminary experiments were performed where bellows were used, but because of the difficulties encountered in the filling such a cell, we reverted to the use of the open cell. We have checked the influence of the dissolved compressed gas, on one hand, by a simple calculation which shows that the effect is negligible, and on the other hand, by performing experiments with argon and nitrogen successively. Experiments showed no difference in melting points observed at a given pressure. Such a conclusion had some time ago been pointed out by Bridgman [7]. At the lower part of the cell, a finger-shaped tube was soldered which protruded into the cell. It contained a Pt/Pt-10% Rh thermocouple for the measurement of the melting temperature. The radial temperature gradient was measured with two Pt/Pt-10% Rh thermocouples mounted in opposition between the top of the inner tube and the point at the same level in a metal shell surrounding the cell. Three control thermocouples (Nisil–Nicrosil) were arranged along the cell to measure and correct for longitudinal temperature gradients. Two quantities were recorded simultaneously on the two channel recorder: the temperature of the sample and the radial temperature gradient between the sample and the shell. To ensure that the beginning of freezing occurred as close as possible to the measuring point, it was necessary for the temperature of the upper part of the cell to be slightly higher than the one of the lower part. The design of the furnace allowed such a control. The filling of the cell was made in a glove box under argon.

The amount of salt which was used was about 12 g. The cell was about 60 mm long and 15 mm in internal diameter.

4. DESCRIPTION OF AN EXPERIMENT

At a fixed pressure, that of the compressing gas, the sample was heated to a temperature above its melting point. To ensure a complete melting, the temperature was stabilized around a fraction of a degree above the assumed melting temperature. Then the sample was cooled very slowly. The decrease in temperature was controlled with an adjustable heating power system. The decrease in temperature was about $1 \ K \cdot min^{-1}$. Theoretically, during freezing, a perfect horizontal plateau should be observed corresponding to the freezing temperature. In reality, the recorded curves were not always so perfect. However, as is shown in the case of LiOH in Fig. 1, the freezing plateau can be correctly defined after the observation of a small supercooling (curve 1). Curve 2 defines the radial gradient, and yields supplementary information, analogous to DTA, and specifies the beginning
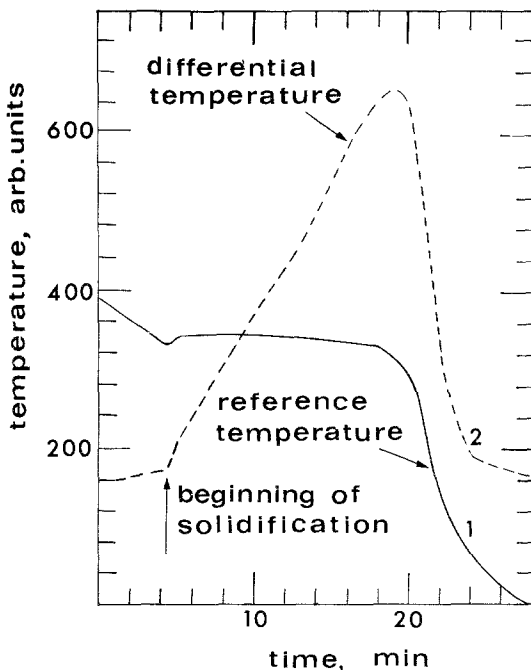

Fig. 1. Recording of one melting temperature for LiOH.

of melting. In general, the reproducibility of these observations leads to the determination of the melting temperature with an error less than 0.5 K. For two systems ($NaNO_2$–$NaNO_3$–KNO_3 and $NaCl$–$MgCl_2$), the records of the melting plateau deviate from theoretical behavior. However, in both cases, the shape of the recorded curves leaves no doubt of the presence of the mechanism of freezing without displacement of composition.

5. EXPERIMENTAL RESULTS

5.1. Choice of Substances

The substances, such as LiOH and the mixture $NaCl$-$MgCl_2$, which were selected for this study, are often sensitive to the presence of water, even in a small quantity. For this reason all the preparations were made in a glove box under dry argon. The basic products were as pure as sold by the chemical product companies. Before their use they were melted and crystallized under vacuum. The mixtures were made by weighing in a glove box. Only LiOH was purified following the process indicated by Rollet et al. [8]. Nevertheless, the melting point found at atmospheric pressure was low and can be explained by the presence of Li_2CO_3, which is a source in the preparation of LiOH.

5.2. Analysis of the Data

The slope $(dT/dP)_m$ of the liquid-solid coexistence curve, and especially the slope at the origin, was the main outcome of this study. Therefore, instead of the theoretical equations describing the function $T_m = f(P)$, it appears preferable to fit the experimental values with spline functions. The error on the volume change was analyzed according to the relation

$$\frac{\delta(\Delta V_m^0)}{\Delta V_m^0} = \frac{\delta(\Delta S_m^0)}{\Delta S_m^0} + \delta\left(\frac{dT}{dP}\right)_m^0 \bigg/ \left(\frac{dT}{dP}\right)_m^0 \tag{1}$$

The error in ΔS_m^0 is the most significant one, but is well defined. It varies from 1 to 5% depending on the source of the data in the literature. The reproducibility of the temperature varies from 0.15 to 0.60 K. The error in the slope is more difficult to assess; it can be determined graphically. In order to take into account the statistical effect of the number of measurements, it is reasonable to divide the error by the number of degrees of freedom for a series of data. Even so, the error is larger because it would be necessary to take into account the statistical effect on each point of the curve $T_m = f(P)$.

5.3. NaNO₃

Although the solubility process is probably different from one salt to another, we checked the influence of the compressing gas on the melting temperature of $NaNO_3$. An earlier calculation by Bridgman [7] had shown that dissolved gases do not significantly lower the melting temperature. It may be noted that our measurements are in excellent agreement with the results obtained by various investigators and various methods where the salt was not in contact with the compressing gas [4, 9, 10]. Also, two series of experiments performed with argon and nitrogen have yielded identical results. Our experimental results on $NaNO_3$ are reported in Table I and Fig. 2.

The values of enthalpy of melting $NaNO_3$ found in the literature vary from 14.2 to 15.6 kJ · mol^{-1} [11–15]. The difficulty of this measurement arises from the existence of a transition between ordered and disordered rhombohedral phases [16] around 275°C, which is about 30 K below the melting temperature. In Fig. 3 we show recent measurements of Denielou et al. [17] by a drop method in an ice calorimeter. We have chosen their value (15.34 ± 0.18 kJ · mol^{-1}) at 307°C to calculate ΔV. The volume change was found to be (3.85 ± 0.08) cm^3 · mol^{-1}; thus $\Delta V / V_s = 9.6\%$ where V_s refers to the volume of the solid at the melting temperature [18]. A comparison of our results of the melting temperature and of the volume change at

Table I. Pressure and Temperature Relationship Along the Melting Curve of $NaNO_3$

Pressure (MPa)	Experimental temperature (°C)	$(dT/dP)_m \times 10^2$ (K · MPa^{-1})
0.1	305.4	14.60
18.6	308.3	14.58
35.4	310.8	14.55
51.0	312.9	14.51
69.9	315.8	14.46
78.3	317.0	14.44
91.0	318.6	14.44
92.5	318.6	14.42
100.6	320.3	14.41
126.6	324.0	14.30
129.5	324.4	14.29
135.2	325.1	14.26
176.5	331.0	14.09
179.6	331.2	14.08
211.0	336.0	14.00
215.0	336.5	13.99
224.3	337.3	—
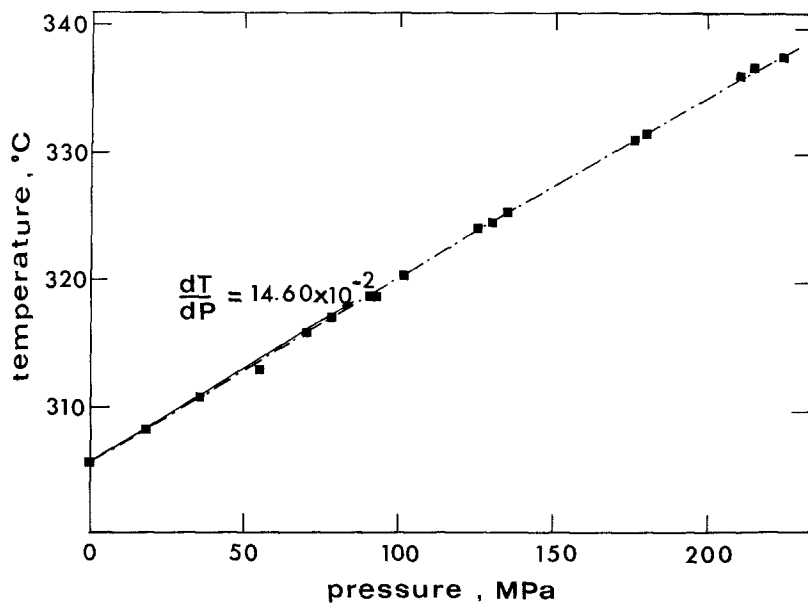
Fig. 2. Melting curve of $NaNO_3$.
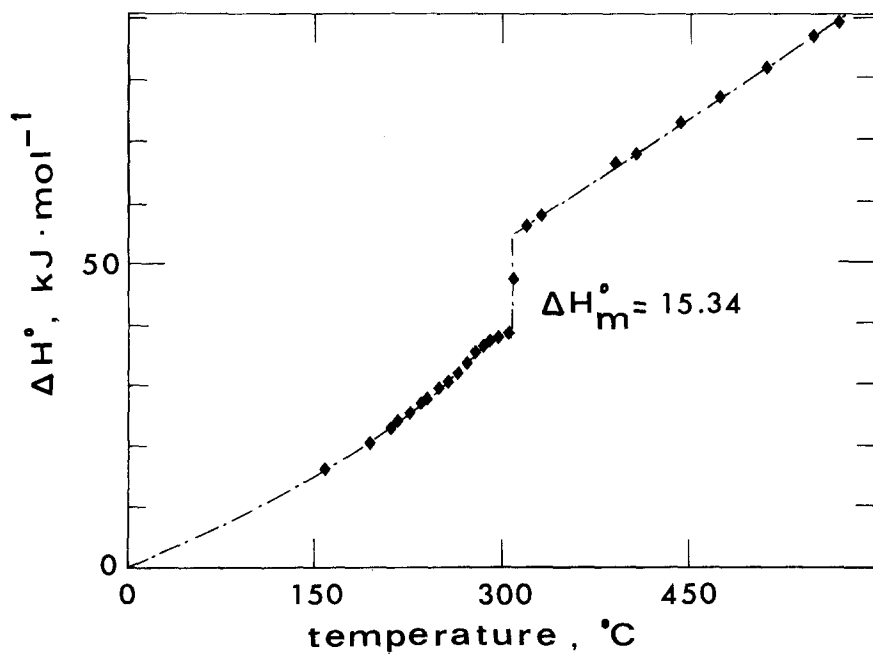
Fig. 3. Variation of the enthalpy of $NaNO_3$.

Table II. Volume Change on Melting of $NaNO_3$

T_m^0 (°C)	$(dT/dP)_m^0 \times 10^2$ (K·MPa^{-1})	$(\Delta V/V_s)_m^0$ (%)	Ref.
306	14.7	9.7	Owens [9]
304.8	15.2	10.0	Schramm and Tödheide [19]
310.6	12.6	8.3	Rapoport [10]
309	15.8	10.7	Schinke and Sauerwald [4]
306	14.6	9.6	Present work

Table III. Volume Change on Melting of Alkali Nitrates

Alkali nitrates	T_m^0 (°C)	$(dT/dP)_m^0 \times 10^2$ (K·MPa^{-1})	$(\Delta V/V_s)_m^0$ (%)
$LiNO_3$[a]	253	14.3	21.4
$NaNO_3$	306	14.6	9.6
KNO_3[a]	333	9.9	3.32
$RbNO_3$[a]	310	−1.46	−0.23
$CsNO_3$[a]	410	37.9	12.7

[a] Ref. [20].

ordinary pressure with those of the literature are given in Table II. The agreement is excellent with those of Owens [9] and Shramm and Tödheide [19], who have used a similar method of measurement but at higher pressures. Our results are slightly different from those of Schinke and Sauerwald [4], who used a dilatometric method. These results justify the validity of our method applied to pure substances. As an indication, we report volume change of the homologous series of alkali nitrates [20] (Table III). The observed differences between the volume changes seem to be uncorrelated.

5.4. LiOH

The interest for this compound is due, in spite of its cost, to its small volume change. The values reported in Table IV show that the melting temperature varies with pressure up to 50 MPa. Above 50 MPa the liquid-solid coexistence curve is practically a horizontal line (Fig. 4), compatible with a null volume change on melting. The above observation confirms that in order to correctly determine the slope at the origin, it is essential to carry out precise measurements close to each other at low pressures. This behavior, which is different from the one observed for $NaNO_3$, of course creates the problem of fitting the melting curve.

Table IV. Pressure and Temperature Relationship Along the Melting Curve of LiOH

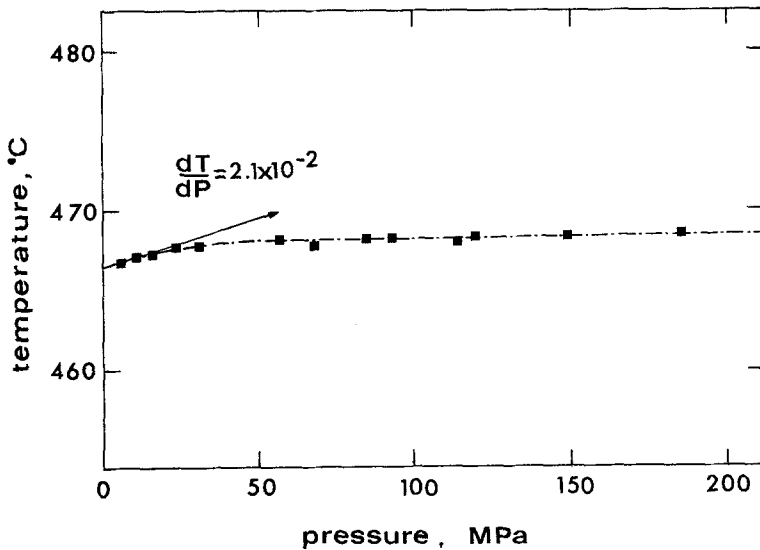| Pressure (MPa)	Experimental temperature (°C)	$(dT/dP)_m \times 10^2$ (K $\cdot$ MPa^{-1})
0.1	466.7	2.08
5.0	466.9	2.08
10.2	467.4	2.04
15.3	467.3	1.98
22.5	467.7	1.86
30.0	467.9	1.69
55.5	468.2	1.07
66.7	468.4	0.85
84.2	468.2	0.59
91.8	468.4	0.49
112.5	468.1	0.34
119.0	468.3	0.33
148.2	468.5	0.24
184.4	468.5	0.13
213.9	468.5	0.14

Fig. 4. Melting curve of LiOH.

Published values of the melting point at atmospheric pressure extend from 445°C [21] to 477°C [22,23]. These deviations are caused by the quality of the samples, which are very sensitive to impurities and humidity. The heat of melting is 20.9 kJ · mol^{-1} [24]. The volume change ΔV is 0.6 ± 0.05 cm^3 · mol^{-1}; then $\Delta V / V_s = 3.5\%$. We note the large error in the slope $(dT/dP)_m$ that results from the shape of the melting curve, which is practically horizontal. In the literature, we found the value $\Delta V \simeq 0.1$ cm^3 · mol^{-1} determined by the recording of dilatometric curves of the solid and the liquid [2].

5.5. Na$_2$SO$_4$–NaCl (0.35–0.65 M)

With a melting temperature of 623°C, the mixture offers little interest for energy storage. However, it is a simple eutectic, which behaves as an ideal solution as was confirmed by the studies of Klotchko [25], Walters [26], and Flood et al. [27]. According to these investigators, the melting temperature is located between 615.6°C [28] and 628°C [25] at atmospheric pressure. We selected this mixture to study the behavior of a eutectic under pressure, for a possible change of composition of the eutectic mixture under pressure. In the limit of compression that we reached, we did not observe a change in the recordings showing the beginning of the crystallization of either one of the pure salts. This justifies the extension of the method based on the Clapeyron equation to the study of volume changes on the melting transition of eutectic mixtures at low pressures. The results are reported in Table V and shown in Fig. 5. The enthalpy of melting was calculated from enthalpies of melting of NaCl [29] and Na$_2$SO$_4$ [30] and was found to be 19.9 kJ · mol^{-1}. The volume change, 4.5 ± 0.4 cm^3 · mol^{-1},

Table V. Pressure-Temperature Relationship Along the Melting Curve of
Na$_2$SO$_4$–NaCl

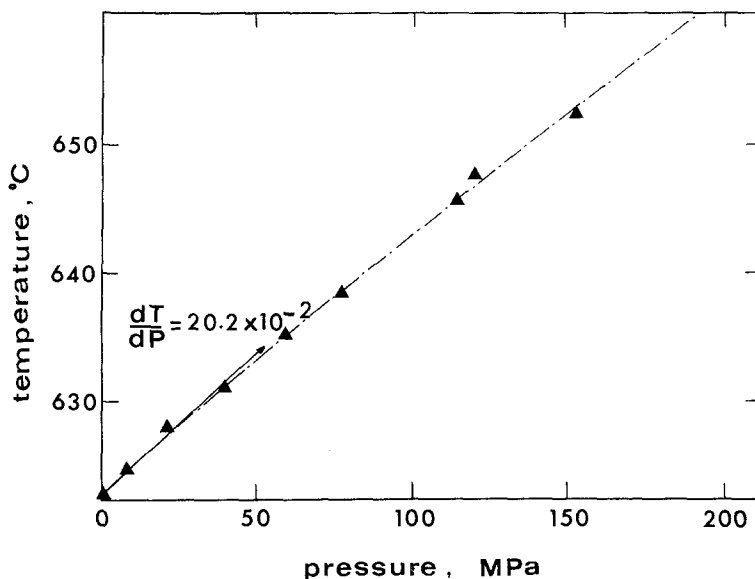| Pressure (MPa)	Experimental temperature (°C)	$(dT/dP)_m \times 10^2$ (K · MPa^{-1})
0.1	622.6	20.18
7.9	624.8	20.16
20.9	628.0	20.07
40.0	631.1	19.89
58.9	635.2	19.67
77.1	638.3	19.44
114.3	645.5	18.90
119.5	647.6	18.80
152.1	652.2	18.42
221.3	665.3	

Fig. 5. Melting curve of Na_2SO_4–NaCl.

yield to $\Delta V / V_s = 9\% \cdot V_s$ was calculated from the molar volume of pure components, as it was for the other mixtures. The main error arises from calorimetric measurements and was 5 and 1% for the enthalpies of Na_2SO_4 and NaCl, respectively.

5.6. $NaNO_3$–$NaNO_2$–KNO_3 (0.07–0.40–0.53 in weight)

This mixture behaves as a pseudoeutectic in the quaternary system $NaNO_3$–$NaNO_2$–KNO_3–KNO_2 [31]. Although commercialized a long time ago under the name of HITEC, very few measurements have been made after the work of Kirst et al. [32]. In particular, we did not find any measurement of volume change on melting. The experimental values are reported in Table VI and Fig. 6. The entropy of melting is 16.9 $J \cdot mol^{-1} \cdot K^{-1}$ [32]. The volume change ΔV on melting is 1.6 ± 0.08 $cm^3 \cdot mol^{-1}$, yielding $\Delta V / V_s = 4\%$. This small value confirms the fact that HITEC can be used as a heat carrier without any special design of the equipment to take into account accidental cyrstallization.

5.7. Li_2SO_4–NaCl (0.58–0.42 M)

On the phase diagram established by Klotchko [25], the mixture Li_2SO_4–NaCl behaves as an eutectic on the diagonal of the quaternary

Table VI. Pressure-Temperature Relationship Along the Melting Curve of
NaNO$_3$–NaNO$_2$–KNO$_3$

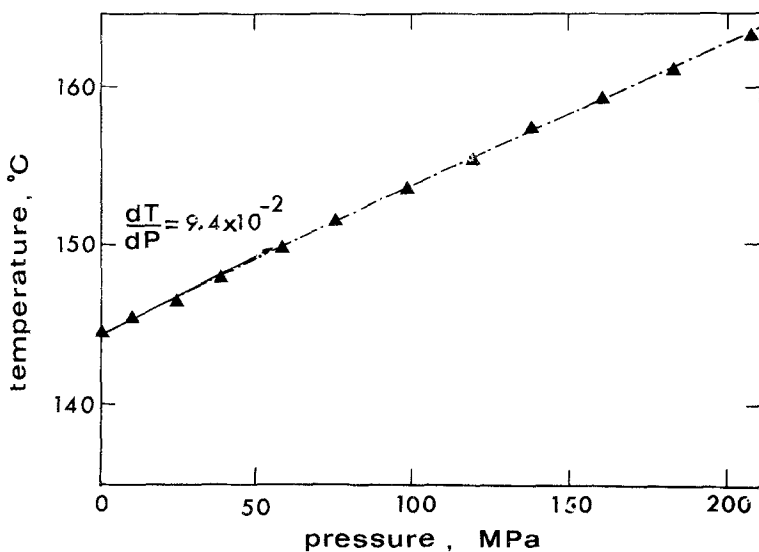| Pressure (MPa)	Experimental temperature (°C)	$(dT/dP)_m \times 10^2$ (K $\cdot$ MPa^{-1})
0.1	144.3	9.40
1.0	144.3	9.40
10.0	145.3	9.40
24.0	146.3	9.39
37.9	147.9	9.37
57.8	149.9	9.31
74.4	151.5	9.23
98.1	153.5	9.11
118.7	155.3	9.00
138.1	157.3	8.90
160.5	159.1	8.81
183.0	160.9	8.76
208.0	163.0	

Fig. 6. Melting curve of NaNO$_3$–NaNO$_2$–KNO$_3$.

Table VII. Pressure-Temperature Relationship Along the Melting Curve of Li$_2$SO$_4$–NaCl

Pressure (MPa)	Experimental temperature (°C)	$(dT/dP)_m \times 10^2$ (K · MPa^{-1})
0.1	490.0	4.2
5.2	490.1	4.2
10.5	490.9	3.99
14.1	490.9	3.97
20.6	491.3	3.92
30.2	491.5	3.82
39.5	492.0	3.71
54.7	492.2	3.52
73.3	493.2	3.25
91.7	493.6	2.97
106.7	493.8	2.75
111.8	494.4	2.67
133.0	494.8	2.38
133.4	494.8	2.36
160.3	495.0	2.17
187.9	495.8	

Na$_2$Cl$_2$–Na$_2$SO$_4$–Li$_2$Cl$_2$–Li$_2$SO$_4$. The heat of melting measured with a drop calorimeter by Clark [33] is 31.2 kJ · mol^{-1}. *A priori*, this value seems to be abnormally high, if we compare it to the heat of fusion of NaCl (27.96 kJ · mol^{-1}) and Li$_2$SO$_4$ (9.3. kJ · mol^{-1}) [34]. In fact the melting temperature is sufficiently low to include the large latent heat of the solid-solid transition of Li$_2$SO$_4$ (575°C, 25.5 kJ · mol^{-1} [34]). From the experimental values reported in Table VII and shown in Fig. 7, the volume variation ΔV was calculated to be 1.7 ± 0.1 cm^3 · mol^{-1}; thus $\Delta V / V_s = 4\%$. This results indicates that this mixture is a good material for energy storage.

5.8. NaCl–MgCl$_2$ (0.60–0.40 M)

From the phase diagram established by Klemm and Weiss [35], there are two defined compounds with noncongruent melting, NaMgCl$_3$ and Na$_2$MgCl$_4$, and the eutectic can be well defined by NaMgCl$_3$ − Na$_2$MgCl$_4$ (0.50–0.50 M). *A priori*, it is not possible to known the behavior of this compound under pressure. On the other hand, the mixture shows an important supercooling which masks partially the real melting. We determined the value 435°C for the melting temperature at ordinary pressure. This value seems low, even if it is sometimes recommended [36]. In this case, the value of the slope of the curve $T_m = f(P)$ in Fig. 8, which is
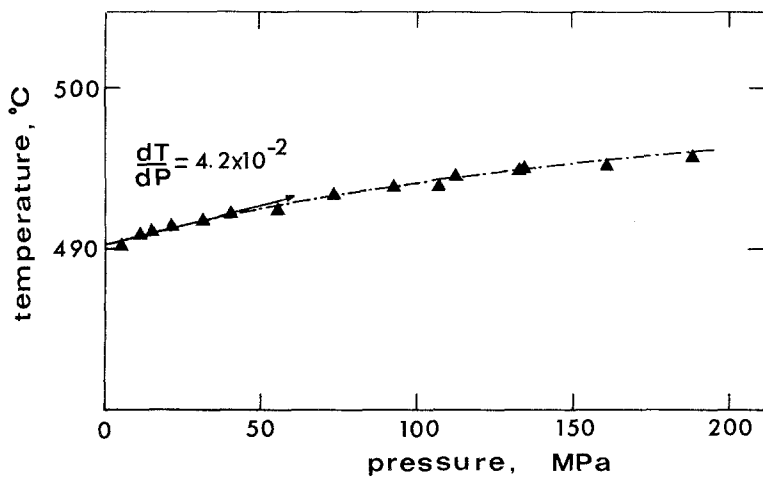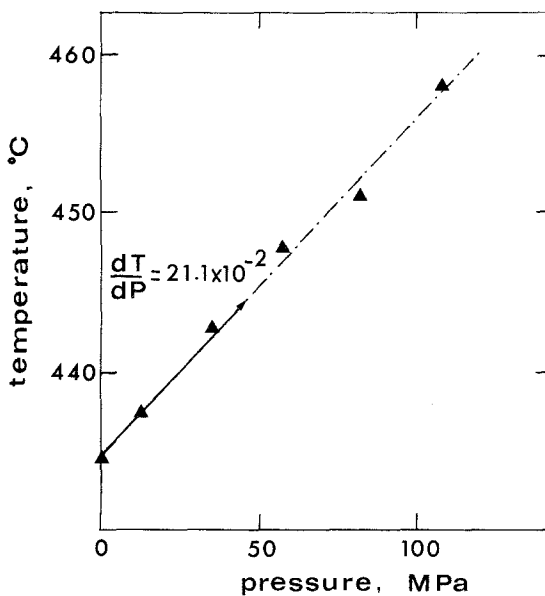
Fig. 7. Melting curve of Li_2SO_4–NaCl.

Fig. 8. Melting curve of NaCl–$MgCl_2$.

Table VIII. Pressure-Temperature Relationship Along the Melting Curve of NaCl–MgCl$_2$

Pressure (MPa)	Experimental temperature (°C)	$(dT/dP)_m \times 10^2$ (K · MPa^{-1})
0.1	434.5	21.14
11.2	437.4	21.14
34.6	442.9	21.07
56.8	447.6	20.98
81.5	451.1	20.96
108.02	458.0	

reported in Table VIII, was found with an error of 11%. The entropy of melting determined in a recent work [3] is 29.6 J · mol^{-1} · K^{-1} (error 2%). Thus the volume change ΔV is 6.3 ± 0.8 cm^3 · mol^{-1} and $\Delta V / V_s = 18\%$. Although less accurate than previous ones, this value indicates a large volume change. It is an important disadvantage of this system for which the cost is low and which was considered as good for mass storage [37].

6. DISCUSSION

The experimental results, including their relative precision, are reported in Table IX. We have shown the advantages of using the method based on the Clapeyron equation over all the other methods in determining the volume change on melting of pure salts and salt mixtures. To the best of our knowledge, there is no theory that deals directly with the prediction of the volume change; thus we will make only a few remarks on the shape of the melting curve from which the slope $(dT/dP)_m^0$ is deduced.

Table IX. Volume Change on Melting of Some Salts and Salt Mixtures

Substance	T_m^0 (°C)	$(dT/dP)_m^0 \times 10^2$ (K · MPa^{-1})	ΔS_m^0 (J · mol^{-1} · K^{-1})	$(\Delta V)_m^0$ (cm^3 · mol^{-1})	$(\Delta V / V_s)_m^0$ (%)
NaNO$_3$	306	14.6 ± 0.09	26.4 ± 0.3	3.85 ± 0.08	9.6
LiOH	467	2.1 ± 0.13	28.2 ± 0.6	0.6 ± 0.05	3.5
Na$_2$SO$_4$–NaCl	623	20.2 ± 0.6	22.2 ± 1.1	4.5 ± 0.4	9
HITEC	144	9.4 ± 0.1	16.9 ± 0.7	1.6 ± 0.1	4
Li$_2$SO$_4$–NaCl	490	4.2 ± 0.1	40.9 ± 0.4	1.7 ± 0.07	4
MgCl$_2$–NaCl	435	21.1 ± 2.3	29.6 ± 0.6	6.3 ± 0.8	18

The equation which is generally used to fit the melting curve is the Simon equation:

$$P/A = \left(T_m/T_m^0\right)^c - 1 \tag{3}$$

where P is the pressure, T_m is the melting temperature at pressure P, and T_m^0 is the melting temperature at atmospheric pressure. A and c are adjustable parameters. Several attempts to justify the Simon equation on a theoretical basis have not been successful. Only the formulation of Ross [38], assuming that spherical molecules interact with a r^{-n} potential, where r is the distance between close neighbors, yields an anlaytical equation similar to the Simon equation:

$$\frac{P}{A} = T^{1+3/n} - 1 \tag{4}$$

In fact, the success of the Simon equation rests on its simple form, close to a polynomial expansion which is well adapted to the mathematical behavior of the liquid-solid coexistence curve when this curve does not show any particular features as is the case for $NaNO_3$. We have noted that a direct determination of the parameters A and c is inaccurate because of the strong correlation between these two parameters. It can be shown that the Simon equation is identical with the Clapeyron equation if the ratio $\Delta H_m/\Delta V_m$ is a linear function of pressure:

$$T\left(\frac{dP}{dT}\right)_m = \frac{\Delta H_m}{\Delta V_m} = a + bP \tag{5}$$

where $A = a/b$ and $b = c$. Then, if the ratio $\Delta H_m/\Delta V_m$ is measured in terms of pressure, the determination of both parameters A and c is straightforward. Unfortunately, no such measurements exist for $NaNO_3$.

Another way to determine A is from its relation to the internal pressure $(\partial U/\partial V)_T$ of the solid [39,40] or the liquid [41] or the difference between the internal pressure of the solid and liquid extrapolated to absolute zero. The value of the internal pressure of liquid $NaNO_3$, extrapolated to absolute zero from the measurments of Sirousse-Zia et al. [42], was found to be $P_I = 1440$ MPa. This value is of the same order of magnitude as the value ($A = 972.5$ MPa) determined by Owens [9]. Considering the value $A = 1440$ MPa, the best fit to the melting curve was obtained for $c = 2.66$.

The Simon equation cannot be used in cases where the melting curve shows a maximum or the substance undergoes a high pressure solid-solid transition, as is probably the case for LiOH. It is reasonable to accept that

the Simon equation or other relations like those of Stishov [43] or Kraut and Kennedy [44] are empirical relations suitable for adequate interpolation of experimental results. It would be inappropriate to use them as predictive equations of the melting behavior of pure salts and salt mixtures.

7. CONCLUSIONS

From a practical point of view, when using the method based on the Clapeyron equation to determine the volume change on melting, we have observed that (the results for LiOH and Li_2SO_4–NaCl mixtures) the slope of the melting curve at atmospheric pressure cannot be obtained accurately from the extrapolation of the high pressure data to atmospheric pressure. In fact, all the necessary information is contained in the data obtained between atmospheric pressure and 50 MPa. The substance Li_2SO_4–NaCl appears to be a good material for energy storage ($\Delta H_m = 354$ kJ $\cdot$ kg^{-1}) with a small volume change on melting. Finally, it was noted that the NaCl–$MgCl_2$ eutectic mixture, despite its low cost and its relatively large ΔH_m ($\Delta H_m = 293$ kJ $\cdot$ kg^{-1}) exhibits a large supercooling and a great sensitivity to humidity. Another disadvantage to its use may be its large volume change on melting.

REFERENCES

1. R. P. Tye, J. G. Bourne, and A. O. Desjarlais, Dynatec Report No. 1503 (1976).
2. G. de Vriet, E. Karig, and G. Drage, *J. Hydronautics* **3**(4S):191 (1963).
3. L. Denielou, J. P. Petitet, and C. Tequi, *Rev. Gén. therm.* **220**:303 (1980).
4. H. Schinke and F. Sauerwald, *Z. Anorg. Allgem. Chem.* **304**:25 (1960).
5. T. G. Kirkwood and I. Oppenheim, *Chemical Thermodynamics* (McGraw-Hill, New York, 1961), p. 118.
6. P. Malbrunot, P. Meunier, and D. Vidal, *High Temp.-High Press.* **1**:93 (1969).
7. P. W. Bridgman, *Phys. Rev.* **3**:126 (1914).
8. A. P. Rollet, R. Cohen-Adad, and J. Choucroun, *Bull. Soc. Chim.*, 146 (1959).
9. B. B. Owens, *J. Chem. Phys.* **48**:2259 (1965).
10. E. Rapoport, *J. Phys. Chem. Sol.* **27**:1349 (1966).
11. H. M. Goodwin and H. T. Kalmus, *Phys. Rev.* **28**:1 (1909).
12. G. J. Janz, F. J. Kelly, and J. L. Perano, *J. Chem. Eng. Data* **9**:1 (1964).
13. W. Dewing, *J. Chem. Eng. Data* **3**:20 (1975).
14. Phuc Nguyen-Duy and E. A. Dancy, *Thermochim. Acta* **39**:95 (1980).
15. K. G. Zeeb, M. G. Lowings, K. G. McCurdy, and L. G. Hepler, *Thermochim. Acta* **40**:245 (1980).
16. F. C. Kracek and E. Posnjak, *J. Am. Chem. Soc.* **53**:1183 (1931).
17. L. Denielou, J. P. Petitet, C. Tequi, M. Fraiha, and D. Sirousse-Zia, to be published.
18. L. Denielou, J. P. Petitet, C. Tequi, and D. Sirousse-Zia, *J. Chim. Phys.* **2**:217 (1977).
19. B. Shramm and K. Tödheide, *High Temp. High Press.* **8**:65 (1976).
20. G. J. Janz, *Molten Salt Handbook* (Academic Press, New York, 1967).
21. De Forcrand, *Ann. Chim. Phys.* **15**:433 (1908).
22. Diogenov, *Dokl. Akad. Nauk. USSR* **78**:697 (1951).
23. Unzhakov, *Dokl. Akad. Nauk. USSR* **87**:791 (1952).

24. W. D. Powers and G. C. Blalock, Rept. ONRL-1653, ITS, US Dept. Commerce, Washington, D.C. (1964).
25. P. A. Klotchko, *Zh. Obshchei. Khim.* **3**:1026 (1953).
26. H. Walters, *Neues Jahrb. Mineral Geol. Beilage* **30**:55 (1910).
27. H. Flood, T. Forland, and A. Nesland, *Acta Chimica Scand.* **5**:1193 (1951).
28. A. Verma, K. E. Johnson, and E. O. Sherman, *Can. J. of Chem. Eng.* **54**:285 (1976).
29. A. S. Dworkin and M. A. Bredig, *J. Phys. Chem.* **64**:969 (1960).
30. L. Denielou, J. P. Petitet, Y. Fournier, and C. Tequi, *C. R. Acad. Sci.* **269**:1577 (1969).
31. S. I. Berul and A. G. Bergman, *Izvest. Sektora Fiz Khim. Anal., Inst. Obshchei Neorg. Khim., Akad Nauk USSR* **25**:233 (1954).
32. W. E. Kirst, W. M. Nagle, and J. B. Castner, *Trans. Am. Inst. Chem. Engrs.* **36**:371 (1940).
33. R. P. Clark, *J. Chem. Eng. Data* **20**:17 (1975).
34. L. Denielou, J. P. Petitet, and C. Tequi, *Thermochim. Acta* **9**:135 (1975).
35. W. Klemm and P. Weiss, *Z. Anorg. Allgem. Chem.* **254**:279 (1940).
36. D. Heine, F. Heess, and D. Steiner, Commission of the European Communities, Contract No. 401-78-1EED-4 (1980).
37. J. J. Nemecek, D. E. Simmons, and T. A. Chub, A Joint Conference 1976 on the American Section of the International Solar Energy Society and the Solar Energy Society of Canada, August 15th/20th, Winnipeg (1976).
38. M. Ross, *Phys. Rev.* **184**:233 (1969).
39. L. Salter, *Phil. Mag.* **45**:369 (1954).
40. C. Domb, *Phil. Mag.* **4**:1316 (1951).
41. S. P. Clark, *J. Chem. Phys.* **31**:1526 (1959).
42. D. Sirousse-Zia, L. Denielou, J. P. Petitet, and C. Tequi, *J. Phys. L.* **38**:L61 (1977).
43. S. M. Stishov, *Sov. Phys., Usp.* **17**:5 (1975).
44. E. A. Kraut and G. C. Kennedy, *Phys. Rev.* **151**:688 (1966).